Improved Radon Based Imaging using the Shearlet Transform

Glenn R. Easley[a], Flavia Colonna[b], Demetrio Labate[c]

[a] System Planning Corporation, Arlington, Virginia
[b] George Mason University, Fairfax, Virginia
[c] North Carolina State University, Raleigh, North Carolina

ABSTRACT

Many imaging modalities, such as Synthetic Aperture Radar (SAR), can be described mathematically as collecting data in a Radon transform domain. The process of inverting the Radon transform to form an image can be unstable when the data collected contain noise so that the inversion needs to be regularized in some way. In this work, we develop a method for inverting the Radon transform using a shearlet-based decomposition, which provides a regularization that is nearly optimal for a general class of images. We then show through a variety of examples that this technique performs better than similar competitive methods based on the use of the wavelet and the curvelet transforms.

1. INTRODUCTION

The concept of Radon transform, originally suggested in 1917 by Johann Radon[1] , is the underlying basis for the development of many of today's imaging sensors. Some of its most famous applications are in the field of computerized tomography (CT) and magnetic resonance imaging (MRI). It also can be used to describe the underlining principles of remote sensing devices such as SAR, inverse synthetic aperture radar (ISAR), and many other sensors that reconstruct an image based on several scans at different locations or angles of a region of interest. In a general sense, the Radon transform projects data onto an appropriate number of lower-dimensional elements which are what is produced from these types of scans. Inverting the Radon transform then produces a reconstruction of the scanned region.

In its classical formulation, the Radon transform can be described abstractly as follows. Let $\mathcal{L}$ be a collection of lines in $\mathbb{R}^2$ whose union is the entire plane. For a function f belonging to the class $L^1(\mathbb{R}^2)$ of functions on $\mathbb{R}^2$ whose modulus is integrable and a line ℓ with slope m and y-intercept b, define

$$(Rf)(m,b) = \int_{-\infty}^{\infty} f(x, mx+b)\, dx.$$

The inversion formula that allows to reconstruct the function f from $g = Rf$ can be written as $f = R^* K g$, where R^* is the a dual transform given by

$$(R^* g)(b,x) = \int_{-\infty}^{\infty} g(m, b-mx)\, dm,$$

and K is the operator given by

$$(Kg)(m,t) = \int_{-\infty}^{\infty} |s| \widehat{g}(m,s) e^{2\pi i s t}\, ds,$$

with

$$\widehat{g}(m,s) = \int_{-\infty}^{\infty} g(m,t) e^{-2\pi i s t}\, dt.$$

Therefore, the Radon inversion formula in operator form is $R^* K R = I$, where I is the identity operator.

The process of inverting the Radon transform can be unstable when the scans are contaminated by noise. Thus, some form of regularization of the inversion is needed in order to control the amplification of noise in

G.R.E.: E-mail: geasley@sysplan.com, F.C.: E-mail: fcolonna@gmu.edu, D.L.: E-mail:dlabate@scsu.edu

the reconstruction. In this work, we propose a technique for regularizing the inversion by means of a multiscale and multidirectional representation known as *shearlets*. Our approach adapts the general framework for the operator–biorthogonal decomposition of the Radon transform originally introduced by Donoho[2] (see also[3]), but allows for a significant performance improvement over the wavelets– and curvelets–based results.

2. SHEARLETS

The theory of composite wavelets, recently introduced in[4–6], provides an effective approach for combining geometry and multiscale analysis by taking advantage of the classical theory of affine systems. In dimension $n = 2$, the *affine systems with composite dilations* are the collections of the form $\{\mathcal{A}_{AB}(\psi)\}$, where $\psi \in L^2(\mathbb{R}^2)$, A, B are 2×2 invertible matrices with $|\det B| = 1$, and

$$\mathcal{A}_{AB}(\psi) = \{\psi_{j,\ell,k}(x) = |\det A|^{j/2}\, \psi(B^\ell\, A^j x - k) :\ j, \ell \in \mathbb{Z}, k \in \mathbb{Z}^2\}.$$

The elements of this system are called *composite wavelets* if $\mathcal{A}_{AB}(\psi)$ forms a *Parseval frame* (also called *tight frame*) for $L^2(\mathbb{R}^2)$; that is,

$$\sum_{j,\ell,k} |\langle f, \psi_{j,\ell,k}\rangle|^2 = \|f\|^2,$$

for all $f \in L^2(\mathbb{R}^2)$. The dilations matrices A^j are associated with scale transformations, while the matrices B^ℓ are associated to area-preserving geometric transformations, such as rotations and shear. This framework allows one to construct Parseval frames whose elements, in addition to ranging at various scales and locations, like ordinary wavelets, also range at various orientations.

In this paper, we will consider a special example of affine systems with composite wavelets in $L^2(\mathbb{R}^2)$, called *shearlets*, where $A = A_0$ is the anisotropic dilation matrix and $B = B_0$ is the shear matrix, which are defined by

$$A_0 = \begin{pmatrix} 4 & 0 \\ 0 & 2 \end{pmatrix}, \quad B_0 = \begin{pmatrix} 1 & 1 \\ 0 & 1 \end{pmatrix}.$$

For any $\xi = (\xi_1, \xi_2) \in \widehat{\mathbb{R}}^2$, $\xi_1 \neq 0$, let

$$\hat{\psi}^{(0)}(\xi) = \hat{\psi}^{(0)}(\xi_1, \xi_2) = \hat{\psi}_1(\xi_1)\, \hat{\psi}_2\left(\frac{\xi_2}{\xi_1}\right), \tag{1}$$

where $\hat{\psi}_1, \hat{\psi}_2 \in C^\infty(\widehat{\mathbb{R}})$, $\operatorname{supp} \hat{\psi}_1 \subset [-1/2, -1/16] \cup [1/16, 1/2]$ and $\operatorname{supp} \hat{\psi}_2 \subset [-1, 1]$. This implies that $\hat{\psi}^{(0)}$ is a compactly-supported C^∞ function with support contained in $[-1/2, 1/2]^2$. In addition, we assume that

$$\sum_{j \geq 0} |\hat{\psi}_1(2^{-2j}\omega)|^2 = 1 \quad \text{for } |\omega| \geq \frac{1}{8}, \tag{2}$$

and, for each $j \geq 0$,

$$\sum_{\ell=-2^j}^{2^j-1} |\hat{\psi}_2(2^j\, \omega - \ell)|^2 = 1 \quad \text{for } |\omega| \leq 1. \tag{3}$$

From the conditions on the support of $\hat{\psi}_1$ and $\hat{\psi}_2$ one can easily deduce that the functions $\psi_{j,\ell,k}$ have frequency support contained in the set

$$\{(\xi_1, \xi_2) : \xi_1 \in [-2^{2j-1}, -2^{2j-4}] \cup [2^{2j-4}, 2^{2j-1}],\ |\xi_2/\xi_1 + \ell\, 2^{-j}| \leq 2^{-j}\}.$$

Thus, each element $\hat{\psi}_{j,\ell,k}$ is supported on a pair of trapezoids of approximate size $2^{2j} \times 2^j$, oriented along lines of slope $\ell\, 2^{-j}$ (see Figure 1(a)).

From equations (2) and (3) it follows that the functions $\{\hat{\psi}^{(0)}(\xi\, A_0^{-j} B_0^{-\ell})\}$ form a tiling of the set

$$\mathcal{D}_0 = \{(\xi_1, \xi_2) \in \widehat{\mathbb{R}}^2 :\ |\xi_1| \geq 1/8,\ |\xi_2/\xi_1| \leq 1\}.$$

Indeed, for $(\xi_1, \xi_2) \in \mathcal{D}_0$

$$\sum_{j\geq 0}\sum_{\ell=-2^j}^{2^j-1} |\hat{\psi}^{(0)}(\xi\, A_0^{-j} B_0^{-\ell})|^2 \quad = \quad \sum_{j\geq 0}\sum_{\ell=-2^j}^{2^j-1} |\hat{\psi}_1(2^{-2j}\,\xi_1)|^2\, |\hat{\psi}_2(2^j\,\frac{\xi_2}{\xi_1} - \ell)|^2 = 1. \tag{4}$$

An illustration of this frequency tiling is shown in Figure 1(b).

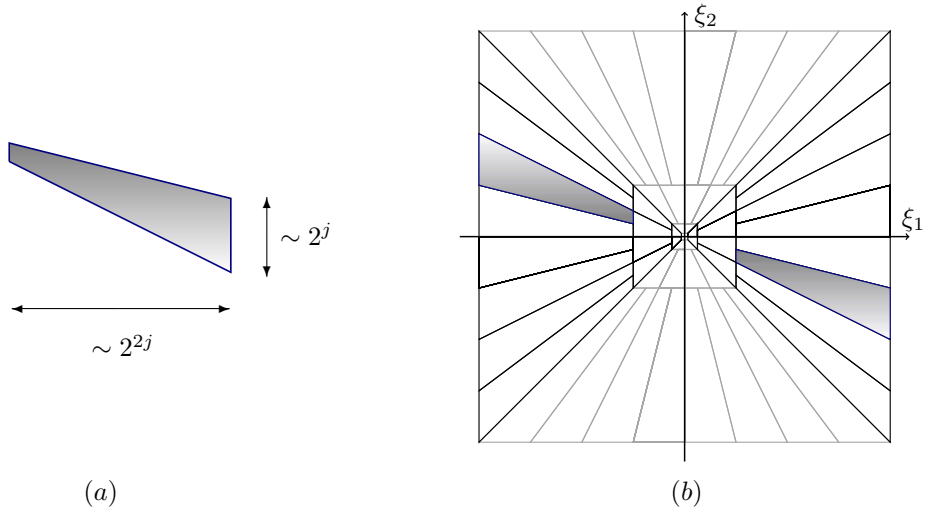

Figure 1. *(a) The frequency support of a shearlet $\psi_{j,\ell,k}$ satisfies parabolic scaling. The figure shows only the support for $\xi_1 > 0$; the other half of the support, for $\xi_1 < 0$, is symmetrical. (b) The tiling of the spatial-frequency plane $\widehat{\mathbb{R}}^2$ induced by the shearlets. The tiling of $\mathcal{D}_0$ is illustrated in black lines; the tiling of $\mathcal{D}_1$ is shown in gray lines.*

Letting $L^2(\mathcal{D}_0)^\vee$ be the set of functions $f \in L^2(\mathbb{R}^2)$ such that the support of $\hat{f}$ is contained in $\mathcal{D}_0$, property (4) and the fact that $\hat{\psi}^{(0)}$ is supported inside $[-1/2, 1/2]^2$ imply that the collection of functions defined by

$$\psi^{(0)}_{j,\ell,k}(x) = 2^{3j/2}\,\psi^{(0)}(B_0^\ell A_0^j x - k), \quad \text{for } j \geq 0, -2^j \leq \ell \leq 2^j - 1, k \in \mathbb{Z}^2, \tag{5}$$

is a Parseval frame for $L^2(\mathcal{D}_0)^\vee$. Similarly, we can construct a Parseval frame for $L^2(\mathcal{D}_1)^\vee$, where $\mathcal{D}_1$ is the vertical cone $\mathcal{D}_1 = \{(\xi_1, \xi_2) \in \widehat{\mathbb{R}}^2 : |\xi_2| \geq 1/8,\, \xi_1/\xi_2| \leq 1\}$. Specifically, let

$$A_1 = \begin{pmatrix} 2 & 0 \\ 0 & 4 \end{pmatrix}, \quad B_1 = \begin{pmatrix} 1 & 0 \\ 1 & 1 \end{pmatrix},$$

and $\psi^{(1)}$ be given by

$$\hat{\psi}^{(1)}(\xi) = \hat{\psi}^{(1)}(\xi_1, \xi_2) = \hat{\psi}_1(\xi_2)\,\hat{\psi}_2\left(\frac{\xi_1}{\xi_2}\right).$$

Then the collection $\{\psi^{(1)}_{j,\ell,k} : j \geq 0, -2^j \leq \ell \leq 2^j - 1, k \in \mathbb{Z}^2\}$ defined by

$$\psi^{(1)}_{j,\ell,k}(x) = 2^{3j/2}\,\psi^{(1)}(B_1^\ell A_1^j x - k) \tag{6}$$

is a Parseval frame for $L^2(\mathcal{D}_1)^\vee$. Details about this can be found in [6].

Finally, let $\hat{\varphi} \in C_0^\infty(\mathbb{R}^2)$ be chosen to satisfy

$$|\hat{\varphi}(\xi)|^2 + \sum_{j\geq 0}\sum_{\ell=-2^j}^{2^j-1} |\hat{\psi}^{(0)}(\xi A_0^{-j} B_0^{-\ell})|^2\, \chi_{\mathcal{D}_0}(\xi) + \sum_{j\geq 0}\sum_{\ell=-2^j}^{2^j-1} |\hat{\psi}^{(1)}(\xi A_1^{-j} B_1^{-\ell})|^2\, \chi_{\mathcal{D}_1}(\xi) = 1$$

for $\xi \in \widehat{\mathbb{R}}^2$, where $\chi_{\mathcal{D}}$ is the indicator function of the set $\mathcal{D}$. This implies that the support of $\hat{\varphi}$ is contained in $[-1/8, 1/8]^2$, $|\hat{\varphi}(\xi)| = 1$ for $\xi \in [-1/16, 1/16]^2$, and the collection $\{\varphi_k : k \in \mathbb{Z}^2\}$ defined by $\varphi_k(x) = \varphi(x-k)$ is a Parseval frame for $L^2([-1/16, 1/16]^2)^\vee$.

Thus, letting $\widehat{\tilde{\psi}}^{(d)}_{j,\ell,k}(\xi) = \widehat{\psi}^{(d)}_{j,\ell,k}(\xi)\, \chi_{\mathcal{D}_d}(\xi)$ for $d = 0, 1$, we have the following result.

THEOREM 2.1.[7] *The collection of shearlets*

$$\{\varphi_k : k \in \mathbb{Z}^2\} \bigcup \{\psi^{(d)}_{j,\ell,k}(x) :\, j \geq 0,\, -2^j + 1 \leq \ell \leq 2^j - 2,\, k \in \mathbb{Z}^2, d = 0, 1\}$$
$$\bigcup \{\tilde{\psi}^{(d)}_{j,\ell,k}(x) :\, j \geq 0,\, \ell = -2^j, 2^j - 1,\, k \in \mathbb{Z}^2, d = 0, 1\},$$

is a Parseval frame for $L^2(\mathbb{R}^2)$.

For $d = 0, 1$, the *shearlet transform* maps $f \in L^2(\mathbb{R}^2)$ into the elements $\langle f, \psi^{(d)}_{j,\ell,k}\rangle$, where $j \geq 0, -2^j \leq \ell \leq 2^j - 1, k \in \mathbb{Z}^2$.

Based on ψ_1 and ψ_2, filters v_j and $w^{(d)}_{j,\ell}$ can be found so that $\langle f, \psi^{(d)}_{j,\ell,k}\rangle = f * (v_j * w^{(d)}_{j,\ell})[k]$[7]. To simplify the notation, we suppress the superscript (d) and absorb the distinction between $d = 0$ and 1 by re-indexing the parameter ℓ so that it has double the cardinality.

3. COMPANION REPRESENTATIONS

For brevity of notation, for $j \geq 0, -2^j \leq \ell \leq 2^j - 1, k \in \mathbb{Z}^2$, we set $\mu = (j, \ell, k)$ and denote $\psi_{j,\ell,k}$ by s_μ. We define new companion representations of the shearlets to be images of a fractional Laplacian as follows.

DEFINITION 3.1. *For a positive rational number* α *and* $f \in C^\infty(\mathbb{R}^2)$, *define* $(-\Delta)^\alpha f$ *by the relation* $\widehat{((-\Delta)^\alpha f)}(\xi) = |\xi|^{2\alpha}\widehat{f}(\xi)$. *Let* $s^+_\mu = 2^{-j}(-\Delta)^{1/4} s_\mu$ *and* $s^-_\mu = 2^j(-\Delta)^{-1/4} s_\mu$.

We may use these companion functions to form a frame that will be used in a construction to invert the Radon transform. First, we establish the following result.

THEOREM 3.2.[8] *The systems* $\{s^+_\mu\}_{\mu\in M}$ *and* $\{s^-_\mu\}_{\mu\in M}$ *are frames for* $L^2(\mathbb{R}^2)$ *which obey the relation*

$$\langle s^+_\mu, s^-_\mu\rangle = 2^{j'-j}\langle s_\mu, s_{\mu'}\rangle, \tag{7}$$

for $\mu, \mu' \in M$, *with* $\mu = (j, \ell, k)$, $\mu' = (j', \ell', k')$.

The following result follows from general facts from frame theory as explained in[3].

COROLLARY 3.1.[8] *The systems* $\{s^+_\mu\}_{\mu\in M}$ *and* $\{s^-_\mu\}_{\mu\in M}$ *satisfy the following conditions:*

1. *(L^2-norm equivalence)*
$$\left\|\sum_\mu \langle f, s^\pm_\mu\rangle\right\|_{\ell^2} \asymp \|f\|_2 \quad \forall f \in L^2(\mathbb{R}^2).$$
2. *There exists* $C > 0$ *such that*
$$\left\|\sum_\mu c_\mu s^\pm_\mu\right\|_{\ell^2} \leq C\left(\sum_\mu c^2_\mu\right)^{1/2},$$
for all $\{c_\mu\} \in \ell^2$.

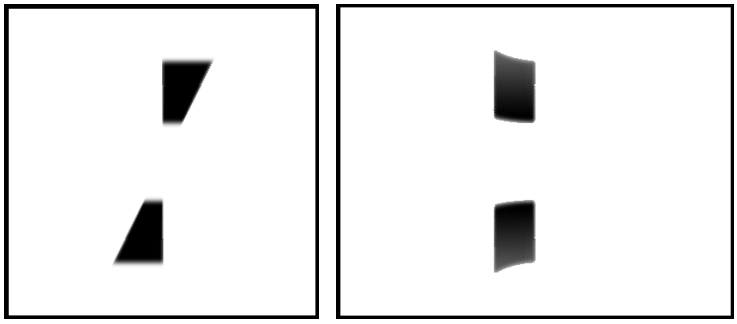

Figure 2. An image of a filter s_μ in the frequency domain on the left. An image of a filter Rs_μ in frequency domain on the right.

4. INVERSION OF RADON TRANSFORM BASED ON SHEARLETS

Having established the frame properties of the companion functions of shearlets, we may now construct an inversion formula of the Radon transform based on them.

Let $\mathcal{D}_R$ be the domain of the Radon transform and observe that all functions $f \in \mathcal{D}_R$ satisfy the symmetry property $Rf(-t, \theta + \pi) = Rf(t, \theta)$.

DEFINITION 4.1. *Given the Radon transform R, the Radon isometry is defined by the formula $\mathcal{R} = (\Delta_1 \otimes I) \circ R$, where*

$$\Delta_1 f(f) = \frac{1}{2\pi} \int_{-\infty}^{\infty} |\omega|^{1/2} \widehat{f}(\omega) e^{i\omega t} \, d\omega,$$

and I denotes the identity operator.

We use the notation $[f, g]$ for the inner product defined on $\mathcal{D}_R$ so that the Radon isometry property can be expressed as $[\mathcal{R}f, \mathcal{R}g] = \langle f, g \rangle$.

Given the Radon isometry function, a set of systems based of the image of the isometry applied to the shearlet companion functions can be used to decompose and invert the Radon transform.

THEOREM 4.2.[8] *The systems $\{U_\mu\}$ and $\{V_\mu\}$ defined by $U_\mu = \mathcal{R}s_\mu^+$ and $V_\mu = \mathcal{R}s_\mu^-$ for $\mu \in M$ are frames for $\mathcal{D}_R$ satisfying the following properties:*

- $\left\| \sum_\mu c_\mu U_\mu \right\|_{\ell^2} \leq C \left(\sum_\mu c_\mu^2 \right)^{1/2}$,
- $\left\| \sum_\mu c_\mu V_\mu \right\|_{\ell^2} \leq C \left(\sum_\mu c_\mu^2 \right)^{1/2}$, *for all* $\{c\}_\mu \in \ell^2$;
- $\sum_\mu \langle f, U_\mu \rangle^2 \asymp \|f\|_{L^2}^2$,
- $\sum_\mu \langle f, V_\mu \rangle^2 \asymp \|f\|_{L^2}^2$, *for all* $f \in \mathcal{D}_R$;
- *(Quasi-biorthogonal relation:)* $[V_\mu, U_{\mu'}] = 2^{j-j'} \langle s_\mu, s_{\mu'} \rangle$;
- $Rf = \sum_\mu \langle f, s_\mu \rangle 2^{-j} V_\mu$;
- $R^* g = \sum_\mu [g, U_\mu] 2^{-j} s_\mu$, *where R^* denotes the adjoint of R.*
- *For all functions f which are finite sums of s_μ's, we have the reproducing formula*

$$f = \sum_\mu [Rf, U_\mu] 2^j s_\mu.$$

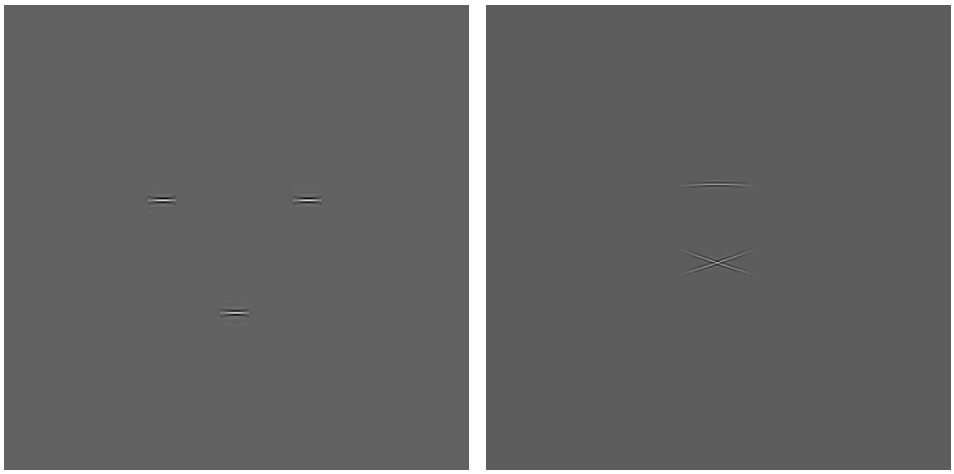

Figure 3. The image on the left illustrates some shearlet coefficients at a given direction and scale. The image on the right shows the corresponding companion shearlet coefficients in a Radon domain.

Note that, defining

$$\Delta_2 f(f) = \frac{1}{2\pi} \int_{-\infty}^{\infty} |\omega| \widehat{f}(\omega) e^{i\omega t} \, d\omega,$$

it is possible to express U_μ and V_μ as $2^{-j}(\Delta_2 \otimes I) R s_\mu$ and $2^j R s_\mu$, respectively. (See [3] for details on this derivation.)

5. INVERSION OF NOISY RADON DATA VIA SHEARLETS.

In our model, we assume that Radon transform data Rf is corrupted by additive white Gaussian noise W; that is, what is received is $Rf + \epsilon W$, where ϵ is measuring the noise level. Projecting this data onto the frame $\{U_\mu\}$, we obtain

$$2^{-j} \langle f, s_\mu \rangle + \epsilon \, n_\mu,$$

where n_μ is a non-i.i.d. (that is, not independent and identically distributed) Gaussian noise ($(n_\mu, n_{\mu'}) = [U_\mu, U_{\mu'}]; \sigma_{n,\mu} = \|s_\mu^+\|_2$). The goal is then to estimate f as

$$\tilde{f} = \sum_\mu T_s([Rf + W, U_\mu] \, 2^j, \tau_j) s_\mu$$

where $T_s(y,t) = \mathrm{sgn}(y)(|y| - t)_+$ is the soft thresholding function and τ_j are scale-dependent thresholds.

6. RESULTS

Several experiments have been carried out that demonstrate the improved performance of a shearlet-based reconstruction. In the first experiment, white Gaussian noise was added to the Radon projections of the Shepp-Logan Phantom image so that a non-regularized reconstruction gave a SNR of 7.48 dB. The reconstructions were then implemented by means of the wavelet, curvelet, and shearlet-based regularization techniques. The standard deviation of the noise for each decomposition level was estimated using a Monte Carlo simulation and the thresholding parameters were chosen to be four times the estimated standard deviation of the noise for the finest decomposition scales and three times the estimated standard deviations of the remain decomposition levels. The results of the reconstructions (shown in Figure 4) had a SNR of 16.64 dB for the wavelet-based estimate, a SNR of 18.73 dB for the curvelet-based estimate, and a SNR of 19.75 dB for the shearlet-based estimate.

It is mathematically known that both the shearlet and curvelet transforms obtain a much better non-linear approximation rate than that of a wavelet transform for star-like domains[7, 9] . Specifically, for this class of images,

a shearlet/curvelet-based estimate yields a MSE approximation rate of $O(\epsilon^{4/3})$ as $\epsilon \to 0$, where ϵ is the noise level of the noisy image[10] , while the MSE approximation rate of wavelet thresholding is $O(\epsilon)$ for $\epsilon \to 0$.

With the above result in mind, we tested the methods using an image that belongs to this class of images (see Figure 5). White Gaussian noise was added to the Radon projections of this star-like image so that a non-regularized reconstruction gave a SNR of 8.02 dB. Using the same thresholding parameters as above, the results of the reconstruction had a SNR of 14.83 dB for the wavelet-based estimate, a SNR of 15.90 dB for the curvelet-based estimate, and a SNR of 16.78 dB for the shearlet-based estimate.

Finally, we tested the performance of the algorithms using an ISAR dataset collected by System Planning Corporation's Mark IV radar of a SAAB 9000 car. A non-regularized reconstruction is shown in Figure 6. Instead of determining the standard deviation of the noise for each decomposition level, we have used a generalized cross validation (GCV) function to determine the thresholding parameters for each band (see [11] for more details). Note that in this case, the curvelet-based estimate is very poor because the downsampling used in its implementation [12] decreases the accuracies in determining the thresholding parameters from the GCV functions.

7. CONCLUSION

We have devised a shearlet-based representation for the purpose of regularizing the inversion of the Radon transform. This representation allows us to obtain noise-reduced reconstructions for many imaging systems such as CT, MRI, SAR, ISAR, and many other sensors that reconstruct an image based on several scans at different locations or angles that can be modeled by the Radon transform. We have shown through various experiments that this method performs significantly better than many of the current competitive techniques. A considerable advantage of our proposed technique is that it is better suited for use with GCV functions for automatic determination of the threshold parameters.

REFERENCES

1. Radon, J., Über die Bestimmung von Funktionen durch ihre Integralwerte längs gewisser Mannigfaltigkeiten, *Berichte Sächsische Akademie der Wissenschaften, Leipzig, Math.–Phys. Kl.*, **69**, 262–267, reprinted in[13] , 177–192, 1917.
2. D. L. Donoho, Nonlinear solution of linear inverse problems by wavelet-vaguelette decomposition, *Appl. Comput. Harmon. Anal.*, **2**, 101–126, 1995.
3. E. J. Candeś, and D. L. Donoho, Recovering edges in ill-posed inverse problems: optimality of curvelet frames, *Annals Stat.*, **30**(3), 784–842, 2002.
4. K. Guo, W. Lim, D. Labate, G. Weiss, E. Wilson, Wavelets with composite dilations, *ERA Amer. Math. Soc.*, **10**, 78–87, 2004.
5. K. Guo, W. Lim, D. Labate, G. Weiss, E. Wilson, The theory of wavelets with composite dilations, in: *Harmonic Analysis and Applications*, C. Heil (ed.), 231–249, Birkhäuser, Boston, 2006.
6. K. Guo, W. Lim, D. Labate, G. Weiss, E. Wilson, Wavelets with composite dilations and their MRA properties, *Appl. Computat. Harmon. Anal.*, **20**, 231–249, 2006.
7. G. R. Easley, D. Labate, and W-Q Lim, "Sparse Directional Image Representations using the Discrete Shearlet Transform," *Appl. Comput. Harmon. Anal.*, **25**(1), 25–46, 2008.
8. G. R. Easley, D. Labate, K. Guo, F. Colonna, Radon Transform Inversion via Shearlets, Preprint, 2009.
9. K. Guo, D. Labate, Optimally Sparse Multidimensional Representation using Shearlets, SIAM J. Math. Anal., **39**, 298–318, 2007.
10. J. L. Starck, E. J. Candès, and D. L. Donoho, "The curvelet transform for image denoising",*IEEE Trans. Image Process.*, **11**(6), 670-684, 2002.
11. V. M. Patel, G. R. Easley, D. M. Healy, Shearlet based deconvolution, Preprint 2008.
12. E. J. Candès, L. Demanet, D. L. Donoho, and L. Ying, "Fast discrete curvelet transforms," *Multiscale Model. Simul.*, **5**(3), 861–899, 2006.
13. Helgason, S., *The Radon Transform*, Progr. Math., **5**, Birkhäuser, Boston, 1980.

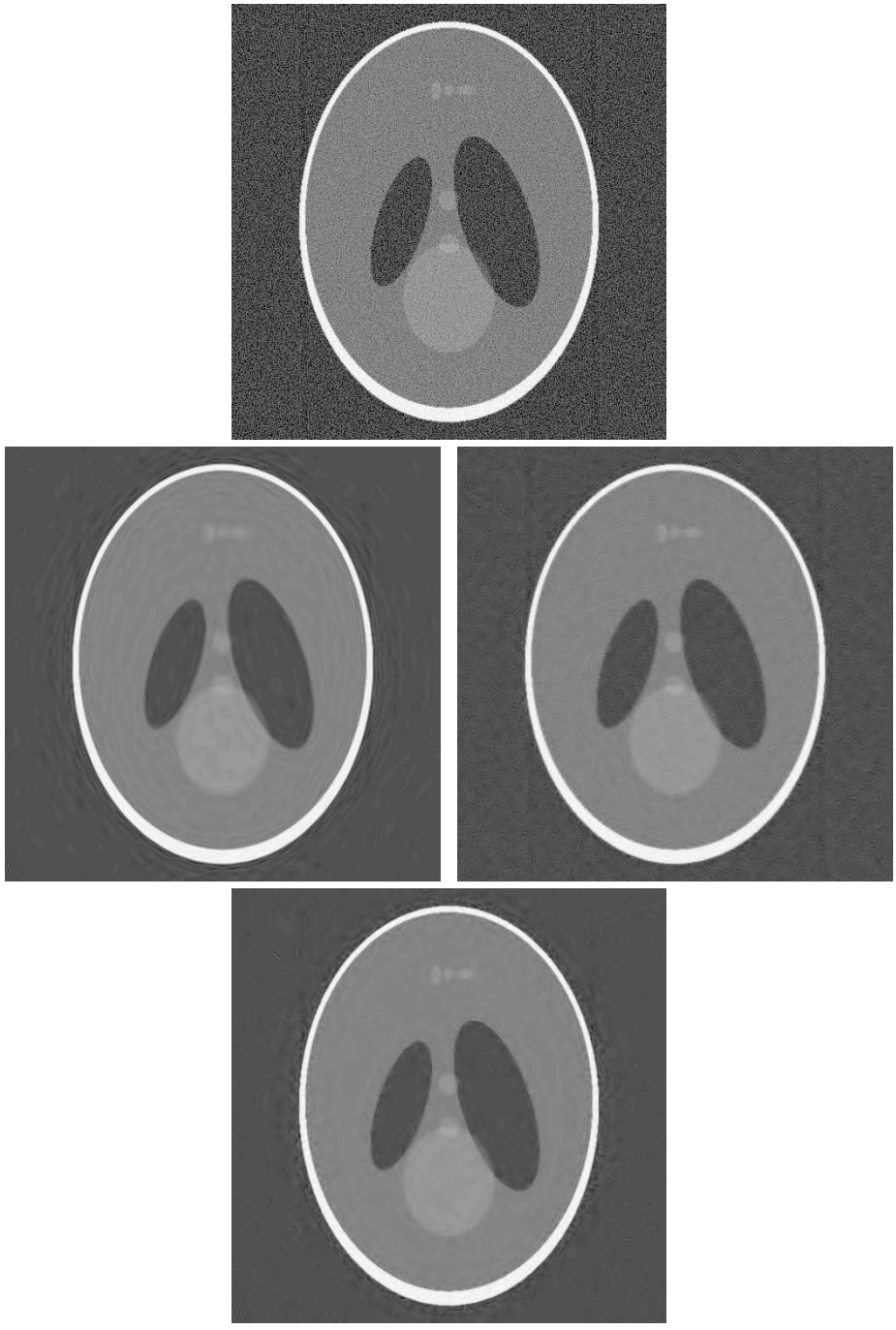

Figure 4. From the top, clockwise: noisy Radon reconstruction (7.48 dB); wavelet-based estimate (16.64 dB); shearlet-Based estimate (19.75 dB); curvelet-based estimate (18.72 dB).

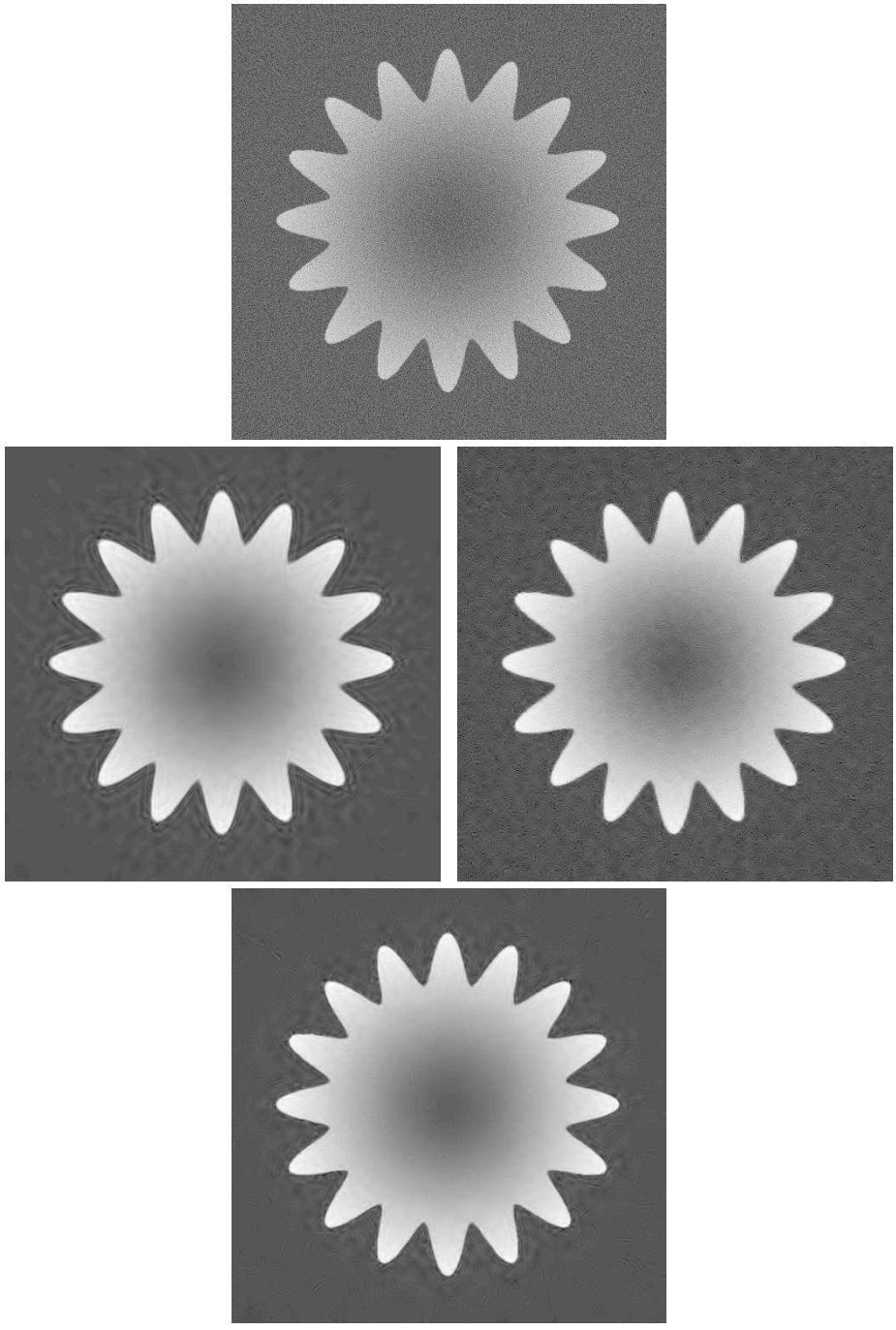

Figure 5. From the top, clockwise: noisy Radon reconstruction (8.02 dB); wavelet-based estimate (14.83 dB); shearlet-Based estimate (16.78 dB); curvelet-based estimate (15.90 dB).

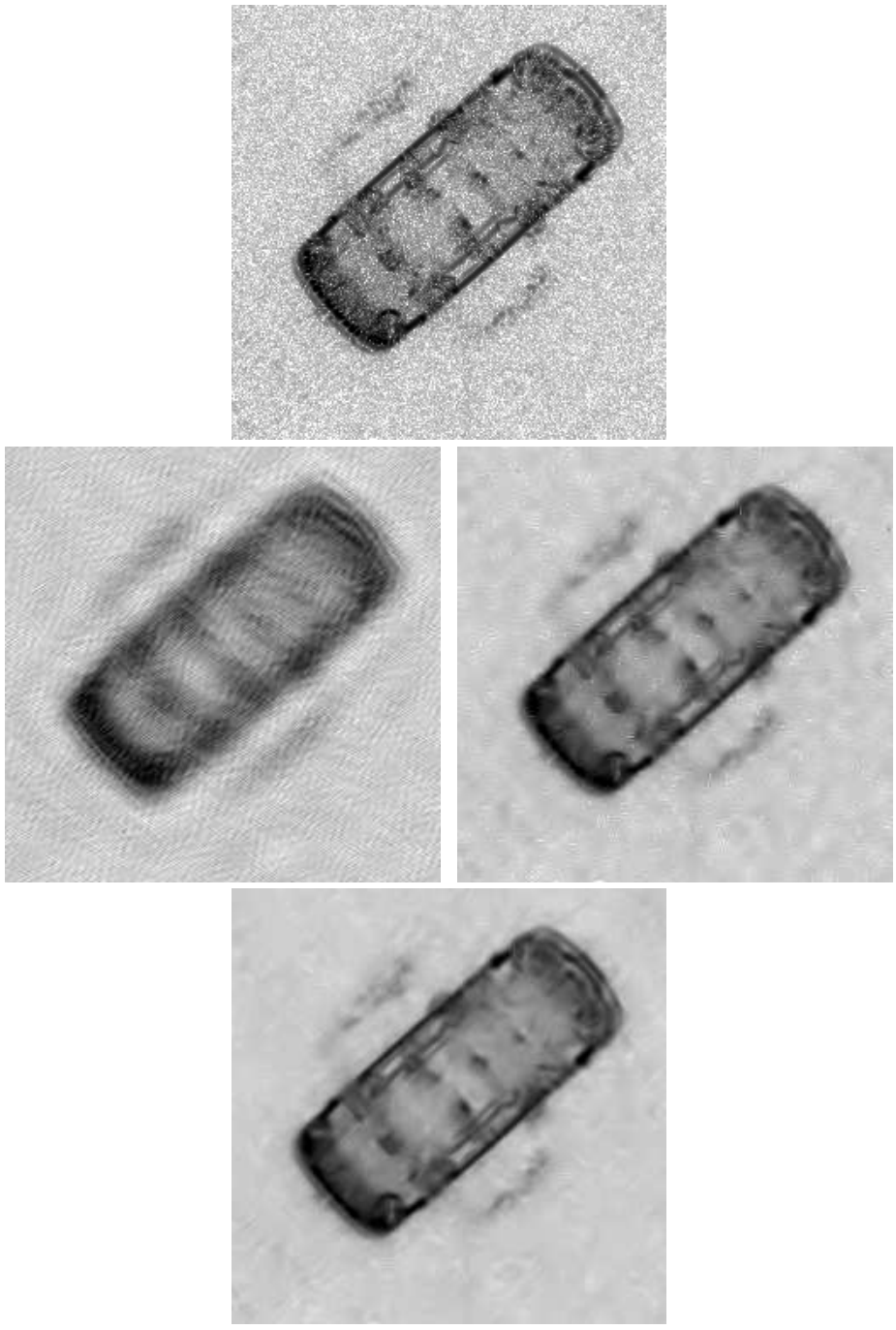

Figure 6. From the top, clockwise: noisy Inverse Synthetic Aperture Radar (Radon) reconstruction; wavelet-based estimate; shearlet-Based estimate; curvelet-based estimate.